HIV reverse transcriptase pre-steady-state kinetic analysis of chain terminators and translocation inhibitors reveals interactions between magnesium and nucleotide 3'-OH

By

Christopher R. Dilmore[1] and Jeffrey J. DeStefano[1,2*]

Keywords: 3'-OH, 3' hydroxyl, HIV reverse transcriptase, magnesium, NRTI, pre-steady-state kinetics

[1]Cell Biology and Molecular Genetics, 3130 Bioscience Research Building, University of Maryland, College Park, MD 20742 USA

[2]Maryland Pathogen Research Institute, College Park, MD 20742 USA

Running Title: 3' hydroxyl is pivotal in physiological Mg^{2+}

* To whom correspondence should be addressed:

Phone: +1 301-405-5449

E-mail: jdestefa@umd.edu

Abstract

Deoxythymidine triphosphate analogs with various 3' groups (-OH (dTTP), -H, $-N_3$, $-NH_2$, -F, $-O-CH_3$, and no group (2′,3′-didehydro-2′,3′-dideoxythymidine triphosphate (d4TTP)), and those retaining the 3'-OH but with 4' additions (4'-C-methyl, 4'-C-ethyl) or sugar ring modifications (D-carba dTTP) were evaluated using pre-steady-state kinetics in low (0.5 mM) and high (6 mM) Mg^{2+} with HIV reverse transcriptase (RT). All analogs showed diminished incorporation compared to dTTP ranging from about 2-fold (3'-H, $-N_3$, and d4TTP with 6 mM Mg^{2+}) to >10-fold (3'-NH_2 and 3'-F with 0.5 mM Mg^{2+}). The exception was 3'-O-CH_3 dTTP which was incorporate profoundly more slowly than other analogs. The incorporation rate (*k*) using 5 μM dTTP and 0.5 mM (free) Mg^{2+} was modestly slower (1.6-fold) than with 6 mM Mg^{2+}, while analogs with 3' modifications were incorporated more slowly (2.8-5.1-fold) in 0.5 mM Mg^{2+}. In contrast, 4'-C-methyl and D-carb, which retain the 3'-OH, were not significantly affected by Mg^{2+}. Consistent with the above results, analogs with 3' modifications were better inhibitors with 6 mM *vs*. 0.5 mM Mg^{2+}, in primer extension reactions on a long template. Equilibrium dissociation constant (K_d) and k_{pol} determinations for dTTP and analogs lacking a 3'-OH indicated that low Mg^{2+} caused a several-fold greater reduction in k_{pol} with the analogs but had little effect on K_d. Overall, results emphasize the importance of as yet undefined interactions between Mg^{2+} and the 3'-OH and indicate that inhibitors with 3'-OH groups may have an advantage in a physiological setting where the concentration of free Mg^{2+} is low.

1. Introduction

Nucleoside Reverse Transcriptase Inhibitors (NRTIs) are a hallmark of Antiretroviral Therapy (ART). All NRTIs currently approved for ART are "chain terminators" and either lack a hydroxyl group at the 3' ribose position, or have a substituted sugar replacing ribose. In either case there is no group present for addition of the next base by reverse transcriptase (RT) (reviewed in: (Holec et al., 2017; Sarafianos et al., 2009; Singh et al., 2010). A second class of emerging NRTIs referred to as "translocation inhibitors" retain the 3'-OH but contain modifications at other positions that dramatically slow the addition of the next base (Kawamoto et al., 2008; Kodama et al., 2001; Michailidis et al., 2009; Ohrui et al., 2006). The first approved HIV drug, azidothymidine (also referred to as Zidovudine, AZT, or ZDV), is essentially dTTP with the 3'-OH replaced by an azido group. Dideoxy drugs replace the 3'-OH with H (including dideoxy inosine (also referred to as Didanosine or ddI) and dideoxy cytidine (a formerly approved HIV drug also referred to as Zalcitabine or ddC). Other drugs remove both the 3'-OH and a hydrogen atom from the 3' position by addition of a carbon double bond to the ribose ring (2',3'-Didehydro-3'-deoxythimidine (also referred to as Stavudine or d4T) and the guanosine analog Abacavir (ABC)). Finally, some approved drugs substantially modify or replace the ribose sugar including Lamivudine (3TC), Emtricitabine (FTC), and Tenofovir (TDF). Despite the success of drugs lacking a 3'-OH, for some translocation inhibitors this group is pivotal in promoting the phosphorylation of the prodrug in cells (Siddiqui et al., 2004).

Others have examined the effect of different groups at the 3' position of thymidine and adenosine analogs for inhibition of HIV RT (Cheng et al., 1987; Herdewijn et al., 1987). For thymidine, inhibition assays using steady-state kinetics and measuring incorporation on poly(rA)-

oligo(dT_{10}) indicated that substitutions of fluorine (F), amino (NH_2), azido (N_3), and hydrogen (H) at the 3' position were all effective inhibitor of dTTP incorporation with modest overall differences, and 3'-F and 3'-N_3 being the most and least effective, respectively (Cheng et al., 1987). Despite this, only the 3'-N_3 derivative (marketed as AZT) has been an effective HIV drug. Drug effectiveness is complicate by several factors including stability, uptake, cellular phosphorylation, target and off-target utilization, and resistance profile among others. Even small modification could potentially affect any of these steps. The F and H 3' substitution (as well as several other changes at other positions) on dATP were also tested for anti-HIV activity and cell toxicity (Herdewijn et al., 1987). Both analogs had lower cytotoxicity than AZT, however, they also had much lower potency. Still, the selectivity index for 3'-H (ddATP) was only about 4.5-fold lower than AZT suggesting it could be an effective drug.

Previous results indicated that the level of Mg^{2+} in *in vitro* reactions can affect the fidelity of HIV RT, efficiency of reverse transcription, and the potency of both NRTIs and Nonnucleoside Reverse Transcriptase Inhibitors (NNRTIs). Fidelity increased significantly (Achuthan et al., 2014; Okano et al., 2018) in reactions performed in low Mg^{2+} (0.25-0.5 mM) that more closely mimics cellular free Mg^{2+} conditions (Delva et al., 1998, 2004; Gout et al., 2014; Gupta et al., 1978; Murphy et al., 1989), in comparison to the high Mg^{2+} (~6 mM) typically used in *in vitro* reactions with RT. The efficiency of reverse transcription, as judged by the length of products produced in primer extension reactions, was greater with physiological Mg^{2+} concentrations (Goldschmidt et al., 2006). The effect on NRTIs and NNRTIs was opposite, with the former being less effective in low Mg^{2+} and the latter being more effective (Achuthan et al., 2017; Goldschmidt et al., 2006).

In this report we used pre-steady-state kinetic analysis at a fixed nucleotide concentration (5 μM) that approximated cellular dNTP concentrations (Amie et al., 2013; Diamond et al., 2004; Kennedy et al., 2010), and high (6 mM) or low (0.5 mM) Mg^{2+} concentrations to examine the incorporation rate of dTTP and several dTTP analogs with substitutions at the 3' position. This included 3'-OH (dTTP), N_3 (AZT), NH_2, F, O-CH_3, H (ddTTP), and d4T (no group at this position). Three translocation type dTTP analog inhibitors (4'-C-methyl, 4'-C-ethyl, and D-carba dTTP) that retained the 3'-OH were also tested. Determinations of k_{cat} and K_d were also performed for some analogs under pre-steady-state conditions. Incorporation rates at 5 μM varied depending on the 3' and 4' substitution. The incorporation rate of analogs that retained the 3'-OH, except for 4'-C-ethyl dTTP, was not significantly affected by Mg^{2+} concentration. All other analogs were between 2.8- and 5.1-fold slower with low Mg^{2+} than with high, while the natural nucleotide, dTTP, was only 1.6-fold slower in low Mg^{2+}. All 3' and 4' substitutions (and D-carba) showed reduced incorporation rates compare to dTTP at both low and high Mg^{2+} with the noted exacerbation at low Mg^{2+}. However, while 3'-O-CH_3 dTTP was incorporated profoundly more slowly than dTTP, all other analogs showed less than ~15-fold diminished incorporation rates and most were effective inhibitors in extension assays on a heteropolymeric template. These results illustrate the potential benefit for NRTI drugs with 3'-OH groups, especially under physiological Mg^{2+} concentrations, while also promoting a direct or indirect interaction between the 3'-OH of incoming nucleotides and Mg^{2+}.

2. Materials and Methods

Materials. 3'-fluor (F) and 3'-O-methyl (O-CH_3) dTTP were synthesized by AX Molecules Inc., San Marcos, CA. 3'-amino (NH_2) dTTP and dideoxy TTP (ddTTP) were from TriLink Bio Technologies. AZTTP and d4TTP were from Sierra Bioresearch, Tucson, AZ. 4'-C-methyl, 4'-C-ethyl, and D-carba dTTP (Boyer et al., 2007; Boyer et al., 2009)were a generous gift from Dr. Stephen Hughes (National Institutes of Health). All other nucleotides were from Roche Diagnostics Corporation. All nucleotides had purity levels >95% (as determined by mass spectroscopy and TLC analysis). T4 polynucleotide kinase (PNK) was from New England Biolabs. Radiolabeled compounds were from PerkinElmer. DNA oligonucleotides were from Integrated DNA Technologies (IDT). G-25 spin columns were from Harvard Apparatus. All other chemicals were obtained from Fisher Scientific, VWR, or Sigma.

Preparation of HIV reverse transcriptase (HIV RT). The expression plasmids (pRT66 and pRT51) for HIV-1 RT (HXB2 sequence) were a generous gift from Dr. Michael Parniak (Professor Emeritus, University of Pittsburgh) (Fletcher et al., 1996). The enzyme, which is a non-tagged heterodimer consisting of equal proportions of p66 and p51, was prepared as described (Hou et al., 2004).

Preparation of primer-templates for pre-steady-state kinetics and inhibitor analysis on 100 nucleotide template. For pre-steady-state kinetics, 5'-^{32}P-labeled 20-nucleotide primer (5'-TTCCCGTCAGCCTAGCTGAG-3′) and 36-nucleotide template (5'-ATCGTCGTACTCAGCTAGGCTGACGGGAAATTGTAT-3′) were mixed at a ratio of 1:1.25 (primer:template) in a buffer containing 50 mM Tris-HCl (pH 8), 80 mM KCl, and 1 mM DTT. For inhibitor analysis during primer extension on a long template (Fig. 4), 5'-^{32}P-labeled 20 nucleotide primer (5′-TTGTTGTCTCTTCCCCAAAC-3′) and 100-nucleotide template (5′-TGGCCTTCCCACAAGGGAAGGCCAGGGAATTTTCTTCAGAGCAGACCAGAGCCAAC

AGCCCCACCAGAAGAGAGCTTCAGGTTTGGGGAAGAGACAACAA-3′) were mixed at a at a ratio of 1:1.5 (primer:template). Hybrids were formed by heating to 80ºC for 5 min then slow cooling in a PCR machine to 4ºC.

Pre-steady-state kinetic parameters for dTTP or dTTP analog incorporation. Experiments were performed using a QFM-4000 from Bio-Logic Scientific Instruments. All experiments were carried out at 37ºC. For each reaction, 20 µL of solution containing 50 nM (in primer) primer-template prepared as described above (final concentration 25 nM in reactions) and 50 nM HIV-1 RT (HXB2) (final concentration 25 nM in reactions) in buffer 1 (50 mM Tris-HCl (pH 8), 80 mM KCl, 1 mM DTT, and 0.5 or 6 mM $MgCl_2$) were loaded into one loop of the apparatus. A second loop contained 20 µL of a solution with various concentrations of dTTP or specific dTTP analogs in the same buffer. Concentrations used ranged from 1 to 100 µM (final concentrations in reaction) for experiments to determine K_d and k_{cat} (depending on the nucleotide) and were 5 µM for pre-steady-state rate (k) determinations with various analogs (see Table 1). For reactions with higher nucleotide concentrations, the starting Mg^{2+} concentration in the 0.5 mM Mg^{2+} reactions were adjusted to keep the free Mg^{2+} concentration at 0.5 mM (Achuthan et al., 2017). A third loop contained 20 µL of a solution containing 0.5 M EDTA (pH 8). Reactions were initiated by rapidly mixing the solutions in loops 1 and 2, then terminated by mixing with loop 3 at time points ranging from 5 milliseconds (ms) to 2 seconds (s). Specific time points depended on the incorporation rate of the individual analogs. All reactions were performed in duplicate and 3 or more independent experiments were used for the values in Table 1. For Table 2 and Fig. 3, at least 2 experiments were used in the plots for each nucleotide concentration, except for the 60 µM d4TTP point which came from a single experiment. The products were mixed with and equal volume of 2X loading buffer (90% formamide, 0.025% each bromophenol blue and xylene cyanol) and resolved on 20%

polyacrylamide-7M urea denaturing PAGE gels as described (Sambrook and Russell, 2001). Gels were dried, then exposed to phosphorimager screens. Quantification was performed using a Fujifilm FLA7000 phosphorimager and Fuji ImageQuant software. First order rate constants for incorporation (*k*) were determined usingSigmaPlot by plotting the concentration of extended starting material vs. time, and fitting the data to a single exponential equation (Johnson, 1995):

$$y = a(1 - e^{-kt}) + C$$

where "a" is the amplitude, *k* is the rate, and "C" is the end point. In some cases, especially for analogs with slower incorporation rates, the data fit better to a simpler equation:

$$y = a(1 - e^{-kt})$$

For some analogs, rate constants at different analog concentrations were used to determine the equilibrium dissociation constant and maximum rate of nucleotide addition (K_d and k_{pol}, respectively) by plotting *k* vs. the concentration of nucleotide and fitting to a hyperbolic equation for ligand binding with single site saturation:

$$y = \frac{B_{max}(x)}{K_d + x}$$

where "B_{max}" corresponds to k_{pol}. Standard error values for K_d and k_{pol} were generated by the program.

Inhibitor analysis during primer extension on a long template. Primer extension reactions were performed to study the inhibition of extension by thymidine analogs as described previously (Achuthan et al., 2017). Briefly, 15 nM 5′-^{32}P-labeled primer was hybridized with 22.5 nM template at a ratio of 1:1.5 as described above. Hybrids were preincubated for 3 min at 37°C in

8.5 µL of buffer 1, all 4 dNTPs and 1 of the analogs (5 µM each and 3 µM, respectively (final concentrations in reactions)) . Extension was initiated by adding 4 µL of HIV RT (final concentration 100 nM) in buffer 1. After extension for 30 min, the reactions were terminated by adding 12.5 µL of 2X gel loading buffer and samples were resolved on an 8% denaturing urea gel and processed as described above.

3. Results

3.1 Substitution of the 3'-OH differentially affects the incorporation rate of dTTP analogs

All the analogs tested, including chain terminators and translocation inhibitors, were incorporated more slowly than dTTP in both 0.5 and 6 mM Mg^{2+} in pre-steady-state assays with 5 µM nucleotide (Table 1, see Fig. 1 for an example of an analysis). This amount was chosen as it approximately mimics the level of nucleotides in dividing T cells (Amie et al., 2013; Diamond et al., 2004; Kennedy et al., 2010). The incorporation rate ordered from highest to lowest in 6 mM Mg^{2+} was 3'-OH > (N_3, no group (d4TTP), H) > (4'-C-methyl, 4'-C-ethyl, NH_2) > (F, D-carba) >> O-CH_3. In 0.5 mM Mg^{2+} the order was 3'-OH > (4'-C-methyl) > (N_3, no group, -H, 4'-C-ethyl, D-carba, NH_2) > F >> O-CH_3. The 3'-O-CH_3 analog was by far the slowest and no data could be obtained using pre-steady-state conditions. However, steady-state analysis showed that the analog could be incorporated by RT (Fig. 2). Among the chain terminating analogs, at 6 mM Mg^{2+}, an N_3, H, or no group at the 3' position were most tolerated. The 3'-F was modestly slower than 3'-NH_2 and the incorporation rate of 3'-O-CH_3 was negligible in comparison (see above). Note that these results agree with a previous steady-state analysis of some of these analogs indicating that they were efficiently incorporated by HIV RT (Cheng et al., 1987) and Introduction). However, the relative

potency of the various inhibitors did not agree with our pre-steady-state analysis or inhibition studies on heteropolymeric template (see Fig. 3 below and the accompanying discussion).

Incorporation rates for translocation inhibitors were less dependent on the Mg^{2+} conditions. Rates for the 4'-C-methyl and 4'-C-ethyl derivatives were similar in 6 mM Mg^{2+} and both were about 3-fold faster than D-carba dTTP. In 0.5 mM Mg^{2+}, only the incorporation rate for 4'-C-ethyl dTTP declined significantly.

3.2 The effect of lower Mg^{2+} on incorporation is largely independent of the type of 3' substitution

All analogs that did not have a 3'-OH were incorporated more slowly in 0.5 than 6 mM Mg^{2+}. The magnitudes of the decreases were in a range between 2.8-5.1-fold (Table 1), with 3'-F and 3'-H (ddTTP) being the lowest and highest, respectively. However, the difference between the various 3' analogs is small and, in most cases, not significant. This indicates that the low Mg^{2+} effect results more from the loss of the 3'-OH than a property of the substitution. The 4'-C-methyl and D-carba translocation inhibitor analogs were not strongly affected by lower Mg^{2+} while dTTP showed just a 1.6-fold decrease in incorporation rate (Table 1). Curiously, 4'-C-ethyl dTTP behaved more like the chain terminators and was incorporated about 3 times more slowly in 0.5 mM Mg^{2+}. It is notable, however, that despite possessing a 3'-OH, 4'-C-ethyl dTTP actually behaves like a chain terminator as unlike 4'-C-methyl and D-carb dTTP, nucleotide cannot be added to this moiety ((Boyer et al., 2007) and see Discussion).

3.3 Analogs without a 3'-OH demonstrate a more profound loss of catalytic efficiency in lower Mg^{2+}

The observed incorporation rate of a nucleotide or analog at a particular concentration is dependent on is affinity for enzyme as well as the overall rate of the catalytic steps. Several reports have shown that 3'-OH substitutions may alter both the binding affinity (i.e. equilibrium dissociation constant (K_d)) for HIV RT as well as the maximum incorporation rate (k_{pol}) (Jamburuthugoda et al., 2005; Kellinger and Johnson, 2011; Kerr and Anderson, 1997; Krebs et al., 1997; Yang et al., 2008). We choose three dNTPs/analogs, dTTP, AZTTP, and d4TTP, to evaluate more thoroughly and determine both pre-steady-state K_d and k_{pol} values at 0.5 and 6 mM Mg^{2+}. Although it would have been more complete to test all 10 analogs, a combination of limiting amounts of material and time made it more feasible to test a smaller representative set. The decision to focus on AZT and d4TTP was made because there is extensive literature on these compounds, and they are approved HIV drugs. The K_d values for all 3 compounds were similar with d4TTP showing a modestly higher K_d than the others at both Mg^{2+} concentrations (Fig. 3 and Table 2). The level of Mg^{2+} did not strongly affect the K_d value for any of the nucleotides. Values for K_d at 6 mM obtained hear were comparable to previous results with high Mg^{2+} (Krebs et al., 1997). As expected from the results in Table 1, changes in k_{pol} were more pronounced, especially for the nucleotides lacking 3'-OH (AZTTP and d4TTP). The decline in catalytic efficiency (k_{pol}/K_d), with 0.5 vs. 6 mM Mg^{2+} was also more pronounced for these analogs. The data again illustrates that the lack of a 3'-OH has a more pronounced negative affect on incorporation in low, more physiological Mg^{2+}, and a decrease in incorporation rate (k) as opposed to changes in affinity (K_d) for the analogs is the predominant factor.

3.4 Inhibition assays on a heteropolymeric DNA template are generally consistent with the kinetic analysis

To evaluate the effectiveness of the various analogs at terminating DNA synthesis, a primer extension assay was performed on a 100 nucleotide DNA template primed with a 20-nucleotide 5'-^{32}P labeled DNA primer (Fig. 4). Assays contained 5 μM dCTP, dGTP, dATP, and dTTP. Analogs were included at 3 μM when present. Consistent with 6/0.5 mM Mg^{2+} ratios shown in Table 1, all chain terminators and 4'-C-ethyl dTTP were less effective (as judged by a lower level of paused (terminated) products and an increase in fully extended products) in 0.5 mM Mg^{2+} compared to 6 mM Mg^{2+}. Among translocation inhibitors, 4'-C-methyl dTTP was essentially equivalent at both 0.5 and 6 mM Mg^{2+} while D-carba was a weak inhibitor under both conditions. The 3'-F analog was the weakest inhibitor among the chain terminators and was also incorporated the slowest in pre-steady-state reactions (Table 1, note that 3'-O-CH_3 produced no inhibition in this assay (data not shown) and its incorporation was not measurable in pre-steady-state reactions (see above)). However, it is important to note that the inhibition observed in these reactions is a function of both incorporation kinetics and binding affinity of the analog for RT vs. binding affinity for dTTP. Therefore, a direct correlation between the results in Table 1 and those in the inhibition assay would not necessarily be expected. Finally, results in Table 1 were performed using a single sequence position on a primer-template while the experiments in Fig. 4 use a long template with positions for thymidine incorporation presented in several sequence contexts.

4. Discussion

In this report, several chain-terminating 3'-OH substitutions of dTTP were tested for incorporation by HIV RT. All the analogs with 3' alterations were incorporated and several (e.g. AZT, ddTTP, and d4T) with only modestly slower rates (~2-fold) than dTTP in 6 mM Mg^{2+}. In

contrast, the rate of incorporation compared to dTTP dropped to ~4.5-16-fold slower (excluding 3'-O-CH_3 which was much slower at both high and low Mg^{2+} (sec. 3.1)) in 0.5 mM Mg^{2+}. This is consistent with previous experiments showing that NRTIs are better inhibitors with higher Mg^{2+} concentrations *in vitro* (Achuthan et al., 2017).

Translocation type inhibitors which retain the 3'-OH behaved more like dTTP in that their rate of incorporation was less affected by low Mg^{2+} (Table 1). However, 4'-C-ethyl dTTP was an exception, showing a 3.1-fold lower rate of incorporation in low Mg^{2+} compared to high. As was noted, this analog behaves more like a chain terminator as it prevents further extension by RT (Boyer et al., 2007). This suggests that the 3'-OH may be in the wrong position for catalysis and this position may also weaken the proposed interactions of the 3'-OH with Mg^{2+}. The translocation inhibitor 4'-ethynyl-2-fluoro-2'-deoxyadenosine triphosphate (EFdATP) is currently in clinical trials. It also binds strongly to HIV RT as the ethynyl group can access a hydrophobic pocket in RT which may stabilize binding (Michailidis et al., 2009; Salie et al., 2016). This, and favorable kinetics lead to EFdATP showing a competitive advantage over the natural dATP nucleotide (Muftuoglu et al., 2014). EFdATP inhibition is also insensitive to Mg^{2+} concentration (Achuthan et al., 2017), and incorporated EFdA can accept addition nucleotides at a highly reduced rate (Muftuoglu et al., 2014). This suggests that translocation inhibitors with the 3'-OH positioned for nucleotide addition behave more like natural nucleotides with respect to Mg^{2+} interactions.

Although positioning of the 3'-OH of an incoming nucleotide is coordinated through many interactions with HIV RT, glutamine 151 (Q151) presumably interacts directly with this group through a proposed hydrogen bond between the amide oxygen from Q151 and the 3'-OH hydrogen atom. Mutations in Q151 like Q151N (glutamine to asparagine) that disrupt this interaction weaken dNTP binding but do not significantly affect k_{pol} (Jamburuthugoda et al., 2005). This

indicates that Q151 likely plays a key role in stabilizing dNTP binding. Dideoxy dTTP which lacks a 3'-OH demonstrated weaker binding to HIV RT than dTTP. However, binding relative to dTTP improved with Q151N which has weakened association with the 3'-OH. This again predicts a role for Q151 in stabilizing binding of dNTPs through interactions with the 3'-OH, as the advantage of a 3'-OH for binding is mitigated when Q151 is altered to a non-interacting amino acid. High divalent cation concentrations can also improve incorporation of analogs without 3'-OH groups with other polymerases, similar to what was found here. The Klenow fragment of *E. coli* polymerase I (KF) discriminates strongly against ddNTPs relative to dNTPs. However, ddTTP incorporation improves in high Mg^{2+} concentrations showing an optimum of 25 mM which is several-fold greater than the optimal concentration for incorporation of dTTP (~2 mM) (Astatke et al., 1998). Like Q151N for HIV RT, an E710A (glutamic acid to alanine) KF mutation reduced ddNTP/dNTP discrimination, consistent with a role for this amino acid in interactions with the 3'-OH. The authors hypothesize that Mg^{2+} may bridge an interaction between KF E710 and the 3'-OH group of incoming nucleotides, although more complex explanations where E710 interacts with Mg^{2+} *via* repositioning of other active site residues cannot be ruled out by the data. It is also not clear if the Mg^{2+} ion in question was metal ion A and/or B, the putative metal ions involved in nucleotide catalysis at polymerase active sites, or another as yet undescribed metal ion. In this regard, it is interesting that a third metal ion has been proposed to be involved in polymerase nucleotide catalysis and may play a role in these interactions (Freudenthal et al., 2015; Freudenthal et al., 2013; Gao and Yang, 2016; Nakamura et al., 2012; Vyas et al., 2015). Interestingly, unlike Q151N, E710A has a larger effect on k_{cat} rather than on binding, leading the authors to postulate that its interaction with the 3′-OH does not contribute to ground state binding. Instead, the data was more consistent for E710-Mg^{2+} interactions having a role in the transition state occurring after

nucleotide binding but before catalysis (Astatke et al., 1998). Our work indicates that lowering the concentration of Mg^{2+} disproportionately depresses the rate of catalysis for all thymidine analogs lacking a 3'-OH without strongly affecting affinity for the limited set (dTTP, AZTTP, and d4TTP) of tested nucleotides (Fig. 3, and Tables 1 and 2). This is consistent with the observations with the KF and suggests that Mg^{2+} may interact with the 3'-OH, either directly or indirectly, in a step after nucleotide binding during the transition state or the chemistry step (the latter was ruled for the KF by demonstrating a lack of a sulfur elemental effect (Astatke et al., 1998), but we did not test this possibility).

It was noteworthy that HIV RT was able to incorporate all 9 analogs that were tested. Only 3'-O-CH_3 dTTP showed very poor incorporation. For chain terminating analogs, there was not a clear consistent chemical property that explained the different rates of incorporation of the analogs. However, electronegative groups that, unlike a 3'-OH, could not donate a H atom for hydrogen bonding (e.g. 3'-F and 3'-O-CH_3) were incorporated the slowest. Groups with potential for positive charge or hydrogen bond formation (e.g. 3'-NH_2, and 3'-N_3), and small groups (e.g. 3'-H (ddTTP) or d4TTP (no group)) were better substrates, although all were less efficiently incorporated than dTTP, especially in low Mg^{2+} (Tables 1 and 2). It is possible that 3'-NH_2 and 3'-N_3 groups may interact with Q151 through charge interactions or H-bonding and this may help compensate for loss of the 3'-OH. Both ddTTP and d4TTP could not establish these interactions but the small size of the 3' substitution and non-charge nature could minimize repulsive interactions. Also, d4TTP is different than the other tested chain terminators as the 2′,3′-didehydro configuration of the sugar moiety alters the structure of the sugar. This makes it more difficult to directly compare it to the other 3′ modified analogs.

It was interesting the 4'-C-ethyl dTTP was clearly a more effective inhibitor than 4' C-methyl or D-carba dTTP at 6 mM Mg^{2+} during extension on the long template (Fig. 4). Even at 0.5 mM Mg^{2+}, where 4'-C-ethyl dTTP was incorporated much more slowly than 4'-C-methyl dTTP and at a rate similar to D-carba dTTP (Table 1), it still was modestly more effective than 4'-C-methyl dTTP and much more effective than D-carba dTTP in the template inhibition assay. This may be due to two factors. First, 4'-C-ethyl dTTP, as stated above, behaves like a chain terminator, and does not allow the addition of other nucleotides after incorporation (Boyer et al., 2007). Additional nucleotides can be added with delayed kinetics with 4'-C-methyl and D-carba dTTP (Boyer et al., 2007; Boyer et al., 2009) and, for these analogs, extended products in the reactions in Fig. 4 may include DNA chains containing more than one inhibitor nucleoside. Second, the K_d for 4'-C-ethyl, 4'-C methyl and D-carba dTTP binding to HIV RT was measured at 6 mM Mg^{2+} in a separate analysis on a different template (manuscript in preparation). The K_d value for D-carba dTTP was ~4-8-fold higher than the others. This helps explain why D-carba dTTP is by far the weakest inhibitor among both translocation and chain terminating inhibitors in the template extension inhibition assay (Fig. 4). It binds more weakly to RT than the other translocation inhibitors, and this, coupled with a relatively low incorporation rate (Table 1), weakens inhibition.

Based on these results, all the tested compounds with the exceptions of 3'-O-CH_3 dTTP could potentially be effective HIV inhibitors. Inhibitors with 3'-OH groups may have an advantage in a physiological setting where the concentration of free Mg^{2+} is low, although current NRTI drugs, none of which possess a 3'-OH, have clearly been effective. Of course, as noted in the Introduction, several other factors are involved in determining inhibitor potency. An example of this is the 3 translocation inhibitors tested here. Only D-carba dTTP (in nucleoside form) is an effective inhibitor of HIV replication in cells (Boyer et al., 2007; Boyer et al., 2009), despite our

findings that it is weaker than 4'-C-methyl or 4'-C-ethyl dTTP in *in vitro* assays. A key reason for the difference is that the D-carba nucleoside can be phosphorylated to triphosphate form much more efficiently than 4' C-methyl or 4'-C-ethyl nucleosides (Boyer et al., 2007; Boyer et al., 2009). Interestingly, adenosine versions of these analogs are strong inhibitors of HIV, owing in part, to more efficient phosphorylation in cells (Vu et al., 2011). This is also an important reason for the high potency of the translocation inhibitor EFdA which couples high affinity for RT with elevated catalytic efficiency and efficient conversion to the triphosphate form (Michailidis et al., 2014).

Acknowledgements

Funding: This work was supported by the National Institutes of Health [grant numbers R01AI150480]. The sponsor was not involved in study design; in the collection, analysis and interpretation of data; in the writing of the report; and in the decision to submit the article for publication.

References

Achuthan, V., Keith, B.J., Connolly, B.A., DeStefano, J.J., 2014. Human immunodeficiency virus reverse transcriptase displays dramatically higher fidelity under physiological magnesium conditions in vitro. J. Virol. 88, 8514-8527.

Achuthan, V., Singh, K., DeStefano, J.J., 2017. Physiological Mg(2+) Conditions Significantly Alter the Inhibition of HIV-1 and HIV-2 Reverse Transcriptases by Nucleoside and Non-Nucleoside Inhibitors in Vitro. Biochemistry 56, 33-46.

Amie, S.M., Noble, E., Kim, B., 2013. Intracellular nucleotide levels and the control of retroviral infections. Virology 436, 247-254.

Astatke, M., Grindley, N.D., Joyce, C.M., 1998. How E. coli DNA polymerase I (Klenow fragment) distinguishes between deoxy- and dideoxynucleotides. J. Mol. Biol. 278, 147-165.

Boyer, P.L., Julias, J.G., Ambrose, Z., Siddiqui, M.A., Marquez, V.E., Hughes, S.H., 2007. The nucleoside analogs 4'C-methyl thymidine and 4'C-ethyl thymidine block DNA synthesis by wild-type HIV-1 RT and excision proficient NRTI resistant RT variants. J. Mol. Biol. 371, 873-882.

Boyer, P.L., Vu, B.C., Ambrose, Z., Julias, J.G., Warnecke, S., Liao, C., Meier, C., Marquez, V.E., Hughes, S.H., 2009. The nucleoside analogue D-carba T blocks HIV-1 reverse transcription. J. Med. Chem. 52, 5356-5364.

Cheng, Y.C., Dutschman, G.E., Bastow, K.F., Sarngadharan, M.G., Ting, R.Y., 1987. Human immunodeficiency virus reverse transcriptase. General properties and its interactions with nucleoside triphosphate analogs. J. Biol. Chem. 262, 2187-2189.

Delva, P., Pastori, C., Degan, M., Montesi, G., Lechi, A., 1998. Intralymphocyte free magnesium and plasma triglycerides. Life Sci. 62, 2231-2240.

Delva, P., Pastori, C., Degan, M., Montesi, G., Lechi, A., 2004. Catecholamine-induced regulation in vitro and ex vivo of intralymphocyte ionized magnesium. J. Membr. Biol. 199, 163-171.

Diamond, T.L., Roshal, M., Jamburuthugoda, V.K., Reynolds, H.M., Merriam, A.R., Lee, K.Y., Balakrishnan, M., Bambara, R.A., Planelles, V., Dewhurst, S., Kim, B., 2004. Macrophage tropism of HIV-1 depends on efficient cellular dNTP utilization by reverse transcriptase. J. Biol. Chem. 279, 51545-51553.

Fletcher, R.S., Holleschak, G., Nagy, E., Arion, D., Borkow, G., Gu, Z., Wainberg, M.A., Parniak, M.A., 1996. Single-step purification of recombinant wild-type and mutant HIV-1 reverse transcriptase. Protein Expr. Purif. 7, 27-32.

Freudenthal, B.D., Beard, W.A., Perera, L., Shock, D.D., Kim, T., Schlick, T., Wilson, S.H., 2015. Uncovering the polymerase-induced cytotoxicity of an oxidized nucleotide. Nature 517, 635-639.

Freudenthal, B.D., Beard, W.A., Shock, D.D., Wilson, S.H., 2013. Observing a DNA polymerase choose right from wrong. Cell 154, 157-168.

Gao, Y., Yang, W., 2016. Capture of a third Mg^{+} is essential for catalyzing DNA synthesis. Science (New York, N Y) 352, 1334-1337.

Goldschmidt, V., Didierjean, J., Ehresmann, B., Ehresmann, C., Isel, C., Marquet, R., 2006. Mg2+ dependency of HIV-1 reverse transcription, inhibition by nucleoside analogues and resistance. Nucleic Acids Res. 34, 42-52.

Gout, E., Rebeille, F., Douce, R., Bligny, R., 2014. Interplay of Mg2+, ADP, and ATP in the cytosol and mitochondria: unravelling the role of Mg2+ in cell respiration. Proc. Natl. Acad. Sci. U. S. A. 111, E4560-4567.

Gupta, R.K., Benovic, J.L., Rose, Z.B., 1978. The determination of the free magnesium level in the human red blood cell by 31P NMR. J. Biol. Chem. 253, 6172-6176.

Herdewijn, P., Pauwels, R., Baba, M., Balzarini, J., De Clercq, E., 1987. Synthesis and anti-HIV activity of various 2'- and 3'-substituted 2',3'-dideoxyadenosines: a structure-activity analysis. J. Med. Chem. 30, 2131-2137.

Holec, A.D., Mandal, S., Prathipati, P.K., Destache, C.J., 2017. Nucleotide Reverse Transcriptase Inhibitors: A Thorough Review, Present Status and Future Perspective as HIV Therapeutics. Curr. HIV Res. 15, 411-421.

Hou, E.W., Prasad, R., Beard, W.A., Wilson, S.H., 2004. High-level expression and purification of untagged and histidine-tagged HIV-1 reverse transcriptase. Protein Expr. Purif. 34, 75-86.

Jamburuthugoda, V.K., Guo, D., Wedekind, J.E., Kim, B., 2005. Kinetic evidence for interaction of human immunodeficiency virus type 1 reverse transcriptase with the 3'-OH of the incoming dTTP substrate. Biochemistry 44, 10635-10643.

Johnson, K.A., 1995. Rapid quench kinetic analysis of polymerases, adenosinetriphosphatases, and enzyme intermediates. Methods Enzymol. 249, 38-61.

Kawamoto, A., Kodama, E., Sarafianos, S.G., Sakagami, Y., Kohgo, S., Kitano, K., Ashida, N., Iwai, Y., Hayakawa, H., Nakata, H., Mitsuya, H., Arnold, E., Matsuoka, M., 2008. 2'-deoxy-4'-C-ethynyl-2-halo-adenosines active against drug-resistant human immunodeficiency virus type 1 variants. Int. J. Biochem. Cell Biol. 40, 2410-2420.

Kellinger, M.W., Johnson, K.A., 2011. Role of induced fit in limiting discrimination against AZT by HIV reverse transcriptase. Biochemistry 50, 5008-5015.

Kennedy, E.M., Gavegnano, C., Nguyen, L., Slater, R., Lucas, A., Fromentin, E., Schinazi, R.F., Kim, B., 2010. Ribonucleoside triphosphates as substrate of human immunodeficiency virus type 1 reverse transcriptase in human macrophages. J. Biol. Chem. 285, 39380-39391.

Kerr, S.G., Anderson, K.S., 1997. Pre-steady-state kinetic characterization of wild type and 3'-azido-3'-deoxythymidine (AZT) resistant human immunodeficiency virus type 1 reverse transcriptase: implication of RNA directed DNA polymerization in the mechanism of AZT resistance. Biochemistry 36, 14064-14070.

Kodama, E.I., Kohgo, S., Kitano, K., Machida, H., Gatanaga, H., Shigeta, S., Matsuoka, M., Ohrui, H., Mitsuya, H., 2001. 4'-Ethynyl nucleoside analogs: potent inhibitors of multidrug-resistant human immunodeficiency virus variants in vitro. Antimicrob. Agents Chemother. 45, 1539-1546.

Krebs, R., Immendorfer, U., Thrall, S.H., Wohrl, B.M., Goody, R.S., 1997. Single-step kinetics of HIV-1 reverse transcriptase mutants responsible for virus resistance to nucleoside inhibitors zidovudine and 3-TC. Biochemistry 36, 10292-10300.

Michailidis, E., Huber, A.D., Ryan, E.M., Ong, Y.T., Leslie, M.D., Matzek, K.B., Singh, K., Marchand, B., Hagedorn, A.N., Kirby, K.A., Rohan, L.C., Kodama, E.N., Mitsuya, H., Parniak, M.A., Sarafianos, S.G., 2014. 4'-Ethynyl-2-fluoro-2'-deoxyadenosine (EFdA) inhibits HIV-1 reverse transcriptase with multiple mechanisms. J. Biol. Chem. 289, 24533-24548.

Michailidis, E., Marchand, B., Kodama, E.N., Singh, K., Matsuoka, M., Kirby, K.A., Ryan, E.M., Sawani, A.M., Nagy, E., Ashida, N., Mitsuya, H., Parniak, M.A., Sarafianos, S.G., 2009. Mechanism of inhibition of HIV-1 reverse transcriptase by 4'-Ethynyl-2-fluoro-2'-deoxyadenosine triphosphate, a translocation-defective reverse transcriptase inhibitor. J. Biol. Chem. 284, 35681-35691.

Muftuoglu, Y., Sohl, C.D., Mislak, A.C., Mitsuya, H., Sarafianos, S.G., Anderson, K.S., 2014. Probing the molecular mechanism of action of the HIV-1 reverse transcriptase inhibitor 4'-ethynyl-2-fluoro-2'-deoxyadenosine (EFdA) using pre-steady-state kinetics. Antiviral Res. 106, 1-4.

Murphy, E., Freudenrich, C.C., Levy, L.A., London, R.E., Lieberman, M., 1989. Monitoring cytosolic free magnesium in cultured chicken heart cells by use of the fluorescent indicator Furaptra. Proc. Natl. Acad. Sci. U. S. A. 86, 2981-2984.

Nakamura, T., Zhao, Y., Yamagata, Y., Hua, Y.-j., Yang, W., 2012. Watching DNA polymerase eta make a phosphodiester bond. Nature 487, 196-201.

Ohrui, H., Kohgo, S., Hayakawa, H., Kodama, E., Matsuoka, M., Nakata, T., Mitsuya, H., 2006. 2'-Deoxy-4'-C-ethynyl-2-fluoroadenosine: a nucleoside reverse transcriptase inhibitor with highly potent activity against all HIV-1 strains, favorable toxic profiles and stability in plasma. Nucleic Acids Symp. Ser. (Oxf), 1-2.

Okano, H., Baba, M., Hidese, R., Iida, K., Li, T., Kojima, K., Takita, T., Yanagihara, I., Fujiwara, S., Yasukawa, K., 2018. Accurate fidelity analysis of the reverse transcriptase by a modified next-generation sequencing. Enzyme Microb. Technol. 115, 81-85.

Salie, Z.L., Kirby, K.A., Michailidis, E., Marchand, B., Singh, K., Rohan, L.C., Kodama, E.N., Mitsuya, H., Parniak, M.A., Sarafianos, S.G., 2016. Structural basis of HIV inhibition by translocation-defective RT inhibitor 4'-ethynyl-2-fluoro-2'-deoxyadenosine (EFdA). Proc. Natl. Acad. Sci. U. S. A. 113, 9274-9279.

Sambrook, J., Russell, D.W., 2001. Molecular Cloning: A Laboratory Manual, 3rd ed. Cold Spring Harbor Laboratory Press, Cold Spring Harbor, NY.

Sarafianos, S.G., Marchand, B., Das, K., Himmel, D.M., Parniak, M.A., Hughes, S.H., Arnold, E., 2009. Structure and function of HIV-1 reverse transcriptase: molecular mechanisms of polymerization and inhibition. J. Mol. Biol. 385, 693-713.

Siddiqui, M.A., Hughes, S.H., Boyer, P.L., Mitsuya, H., Van, Q.N., George, C., Sarafinanos, S.G., Marquez, V.E., 2004. A 4'-C-ethynyl-2',3'-dideoxynucleoside analogue highlights the role of the 3'-OH in anti-HIV active 4'-C-ethynyl-2'-deoxy nucleosides. J. Med. Chem. 47, 5041-5048.

Singh, K., Marchand, B., Kirby, K.A., Michailidis, E., Sarafianos, S.G., 2010. Structural Aspects of Drug Resistance and Inhibition of HIV-1 Reverse Transcriptase. Viruses 2, 606-638.

Vu, B.C., Boyer, P.L., Siddiqui, M.A., Marquez, V.E., Hughes, S.H., 2011. 4'-C-methyl-2'-deoxyadenosine and 4'-C-ethyl-2'-deoxyadenosine inhibit HIV-1 replication. Antimicrob. Agents Chemother. 55, 2379-2389.

Vyas, R., Reed, A.J., Tokarsky, E.J., Suo, Z., 2015. Viewing Human DNA Polymerase beta Faithfully and Unfaithfully Bypass an Oxidative Lesion by Time-Dependent Crystallography. J. Am. Chem. Soc. 137, 5225-5230.

Yang, G., Wang, J., Cheng, Y., Dutschman, G.E., Tanaka, H., Baba, M., Cheng, Y.-C., 2008. Mechanism of inhibition of human immunodeficiency virus type 1 reverse transcriptase by a stavudine analogue, 4'-ethynyl stavudine triphosphate. Antimicrob. Agents Chemother. 52, 2035-2042.

Figure Legends

Figure 1. Example of pre-steady state determination of the rate (*k*) of nucleotide addition with 5 μM dTTP or AZTTP and 0.5 or 6 mM Mg^{2+}. (A) Assays were conducted as described in Materials and Methods with a 20-nt 5'-^{32}P end-labeled DNA primer bound to a 36-nt DNA template using rapid quench analysis. Time points in these assays were 10, 20, 40, 80, 100, 200, and 500 ms and were conducted in duplicate. For nucleotide analogs with slower incorporation rates longer time points were also used. Positions of the primer (P) and primer + 1 nt (P+1) are shown for assays with dTTP and AZTTP at 0.5 or 6 mM Mg^{2+}. FE, full extension; -E, no enzyme added. (B) The data was fitted to an exponential equation as described in Materials and Methods to yield the incorporation rate (k (s^{-1})) used to produce the data in Table 1.

Figure 2. Addition of 3'-O-CH_3 dTTP in steady-state assays with HIV RT with 0.5 or 6 mM Mg^{2+}. Reactions were carried out as described in Materials and Methods using a 20-nt 5'-^{32}P end-labeled DNA primer bound to a 36-nt DNA template. All reactions contained 100 μM 3'-O-CH_3 dTTP with either 0.5 or 6 mM Mg^{2+}. Reactions were carried out for the indicated times and resolved on a 20% denaturing gel. The proportion of extended primer was quantified on a phosphorimager and used to determine the rate (*k*) of nucleotide addition. -E, no enzyme added; P, 5'-^{32}P end-labeled DNA primer; P+1, primer extended with 3'-O-CH_3 dTTP.

Figure 3. Pre-steady state determination of equilibrium dissociation constant (K_d) and k_{pol} for dTTP, AZTTP, and d4TTP. Assays were conducted as described in Materials and Methods with a 20-nt 5'-^{32}P end-labeled DNA primer bound to a 36-nt DNA template using rapid quench analysis. Data points are from independent experiments at various concentrations of dTTP (A), AZTTP (B), or d4TTP (C) (see Fig. 1 for an example). Points from several experiments were

plotted and fit to an equation to determine values as described in Materials and Methods. The indicated values for K_d and k_{pol} are derived from the curve fit program. Values are ± standard errors as determined by the program.

Figure 4. Primer extension on a 100-nt DNA template with HIV RT. Reactions were carried out as described in Materials and Methods using a 20-nt 5'-^{32}P end-labeled DNA primer bound to a 100-nt DNA template. All reactions contained 5 μM dNTPs and 3 μM of the indicated dTTP analog with either 0.5 or 6 mM Mg^{2+}. Reactions were carried out for 30 min and resolved on an 8% denaturing gel. -E, no enzyme added. *d4TTP lane came from another gel and a separate experiment.

Table 1. Comparison of pre-steady state incorporation of dTTP analogs			
[a]Nucleotide ([Mg^{2+}])	[b]k (s^{-1}) ± standard deviation	Relative rate vs. dTTP same [Mg^{2+}]	6/0.5 mM Mg^{2+} with same nucleotide
dTTP (0.5 mM)	8.6 ± 1.3	1	1.6
dTTP (6 mM)	14.1 ± 1.2	1	
Analogs with substitutions at the 3' position (chain terminators)			
ddTTP (0.5 mM)	1.4 ± 0.7	0.16	5.1
ddTTP (6 mM)	7.2 ± 1.0	0.51	
AZT (0.5 mM)	2.0 ± 0.5	0.23	4.5
AZT (6 mM)	8.9 ± 1.9	0.63	
D4T (0.5 mM)	1.8 ± 0.7	0.21	4.6
D4T (6 mM)	8.3 ± 0.8	0.59	
3'-amino dTTP (0.5 mM)	0.81 ± 0.13	0.094	3.8
3'-amino dTTP (6 mM)	3.1 ± 0.1	0.22	
3'-fluoro dTTP (0.5 mM)	0.54 ± 0.13	0.063	2.8
3'-fluoro dTTP (6 mM)	1.5 ± 0.1	0.11	
[c]3'-O-methyl dTTP (0.5 mM)	[c]$3.3 \times 10^{-5} \pm 0.6 \times 10^{-5}$	NA	5.4
[c]3'-O-methyl dTTP (6 mM)	[c]$1.8 \times 10^{-4} \pm 0.2 \times 10^{-4}$	NA	
Analogs with a 3' hydroxyl (translocation inhibitors)			
4'-C-methyl dTTP (0.5 mM)	4.5 ± 1.4	0.52	0.88
4'-C-methyl dTTP (6 mM)	3.9 ± 2.8	0.28	
4'-C-ethyl dTTP (0.5 mM)	1.3 ± 0.1	0.15	3.1
4'-C-ethyl dTTP (6 mM)	3.9 ± 0.4	0.28	
D-carba dTTP (0.5 mM)	1.1 ± 0.5	0.13	1.2
D-carba dTTP (6 mM)	1.3 ± 0.1	0.092	

[a]All nucleotides were tested at 5 µM final concentration. The free Mg^{2+} concentration in reactions is listed (see Methods).

[b]Results are averages from 3 or more independent experiments ± standard deviations. See Fig. 1 for an example of an experiment.

[c]Values for 3' O-methyl dTTP are from steady-state experiments as the rate was too low to reliably measure by pre-steady-state methods. Units are nM/min. They cannot be directly compared to other values for *k*. Conditions were 20 nM primer-template, 20 nM RT, 100 µM 3'-O-methyl dTTP in the same buffer as pre-steady-state reactions and reactions were measured over 30 min.

Table 2. Pre-steady state kinetic data for HIV RT incorporation of TTP, AZTTP, and D4TTP

Nucleotide	$[Mg^{2+}]$ (mM)	[a]k_{pol} (s^{-1})	[a]K_d (μM)	k_{pol}/K_d	[b]Efficiency decline
dTTP	0.5	14.3 ± 0.8	3.3 ± 0.6	4.3	1
AZTTP	0.5	3.3 ± 0.3	5.5 ± 1.7	0.6	7.2
d4TTP	0.5	4.9 ± 0.5	7.6 ± 2.2	0.64	6.7
dTTP	6	25.0 ± 1.3	4.2 ± 0.7	6.0	1
AZTTP	6	17.0 ± 0.6	3.9 ± 0.6	3.9	1.5
d4TTP	6	22.3 ± 1.7	11.6 ± 2.3	1.9	3.2

a- Values were derived from the graphs shown in Fig. 2 and are predicted values base on curve fitting ± standard error (as determined by the fitting program).

b- Numbers represent the fold decline in enzyme efficiency relative to dTTP at the same Mg^{2+} concentration. Enzyme catalytic efficiency was taken as k_{pol}/K_d.

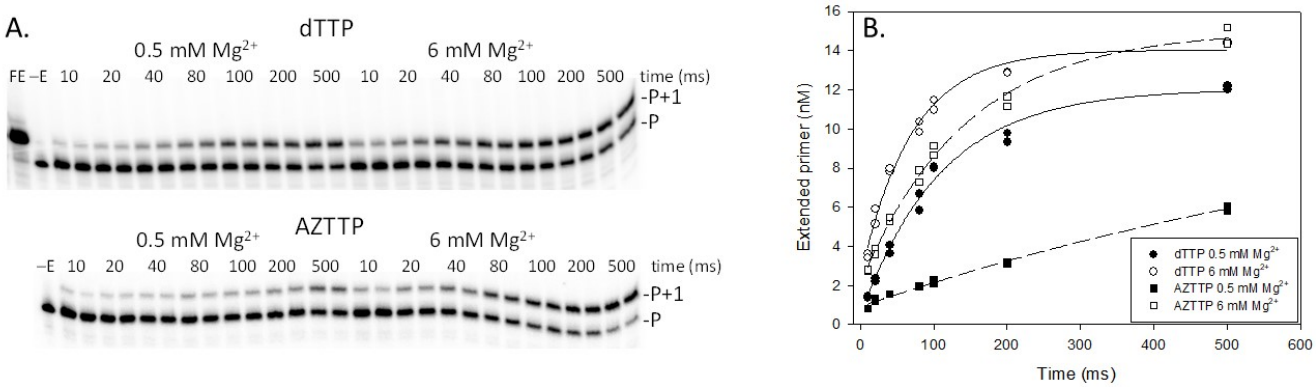

Figure 1. Example of pre-steady state determination of the rate (*k*) of nucleotide addition with 5 μM dTTP or AZTTP and 0.5 or 6 mM Mg^{2+}. (A) Assays were conducted as described in Materials and Methods with a 20-nt 5'-^{32}P end-labeled DNA primer bound to a 36-nt DNA template using rapid quench analysis. Time points in these assays were 10, 20, 40, 80, 100, 200, and 500 ms and were conducted in duplicate. For nucleotide analogs with slower incorporation rates longer time points were also used. Positions of the primer (P) and primer + 1 nt (P+1) are shown for assays with dTTP and AZTTP at 0.5 or 6 mM Mg^{2+}. FE, full extension; -E, no enzyme added. (B) The data was fitted to an exponential equation as described in Materials and Methods to yield the incorporation rate (k (s^{-1})) used to produce the data in Table 1.

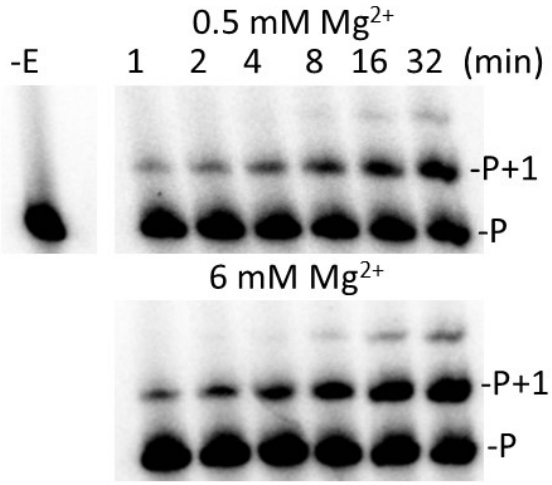

Figure 2. Addition of 3'-O-CH_3 dTTP in steady-state assays with HIV RT with 0.5 or 6 mM Mg^{2+}. Reactions were carried out as described in Materials and Methods using a 20-nt 5'-^{32}P end-labeled DNA primer bound to a 36-nt DNA template. All reactions contained 100 µM 3'-O-CH_3 dTTP with either 0.5 or 6 mM Mg^{2+}. Reactions were carried out for the indicated times and resolved on a 20% denaturing gel. The proportion of extended primer was quantified on a phosphorimager and used to determine the rate (*k*) of nucleotide addition. -E, no enzyme added; P, 5'-^{32}P end-labeled DNA primer; P+1, primer extended with 3'-O-CH_3 dTTP.

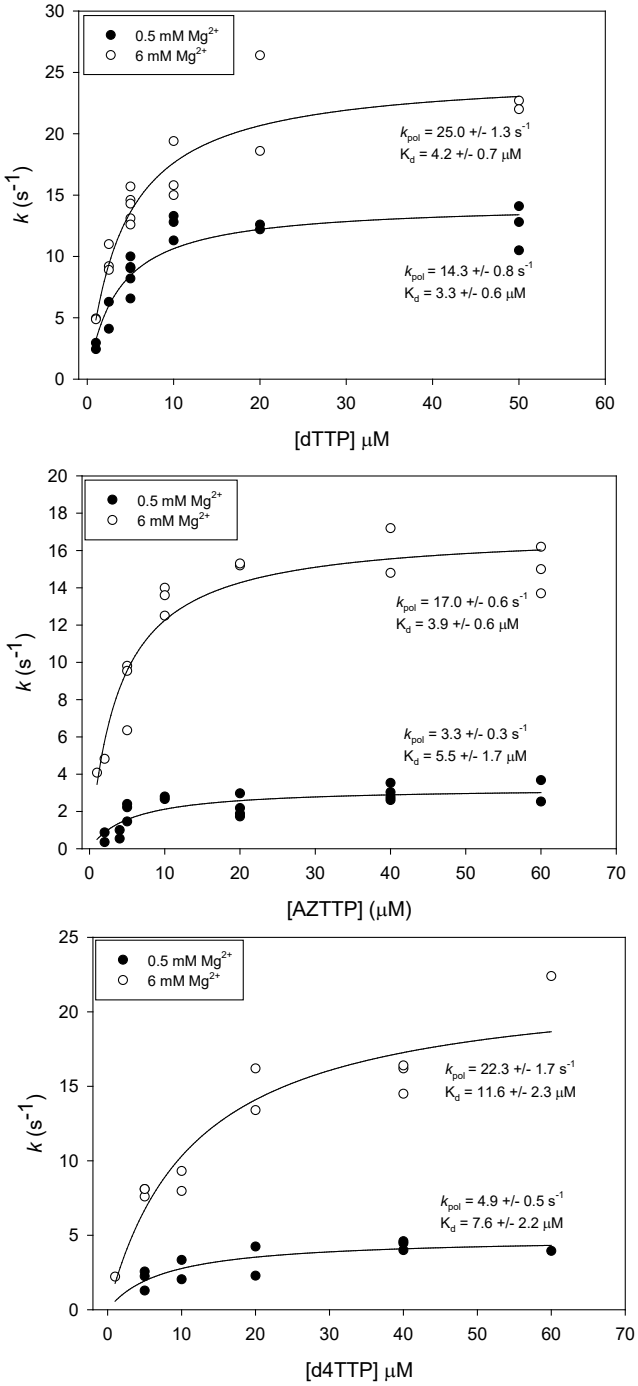

Figure 3. Pre-steady state determination of equilibrium dissociation constant (K_d) and k_{pol} for dTTP, AZTTP, and d4TTP. Assays were conducted as described in Materials and Methods with a 20-nt 5'-^{32}P end-labeled DNA primer bound to a 36-nt DNA template using rapid quench analysis. Data points are from independent experiments at various concentrations of dTTP (A), AZTTP (B), or d4TTP (C) (see Fig. 1 for an example). Points from several experiments were plotted and fit to an equation to determine values as described in Materials and Methods. The indicated values for K_d and k_{pol} are derived from the curve fit program. Values are ± standard errors as determined by the program.

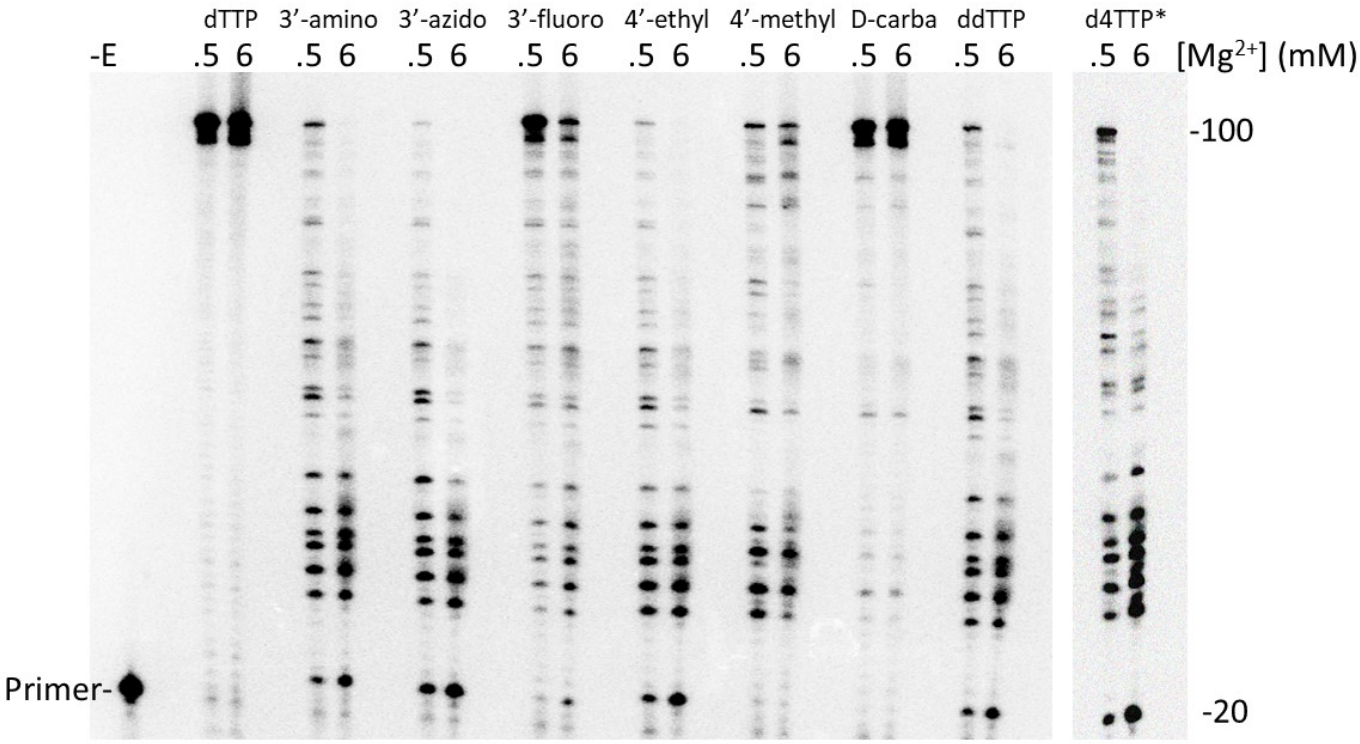

Figure 4. Primer extension on a 100-nt DNA template with HIV RT. Reactions were carried out as described in Materials and Methods using a 20-nt 5'-^{32}P end-labeled DNA primer bound to a 100-nt DNA template. All reactions contained 5 µM dNTPs and 3 µM of the indicated dTTP analog with either 0.5 or 6 mM Mg^{2+}. Reactions were carried out for 30 min and resolved on an 8% denaturing gel. -E, no enzyme added. *d4TTP lane came from another gel and a separate experiment.